UNIVERSITÀ DEGLI STUDI DI TORINO

Phototransformation of the sunlight filter benzophenone-3 (2-hydroxy-4-methoxybenzophenone) under conditions relevant to surface waters

Davide Vione,[a,b]∗ Rosalinda Caringella,[a] Elisa De Laurentiis,[a] Marco Pazzi,[a] Claudio Minero[a]

[a] *Università degli Studi di Torino, Dipartimento di Chimica, Via P. Giuria 5, 10125 Torino, Italy.* *http://www.chimicadellambiente.unito.it*

[b] *Università degli Studi di Torino, Centro Interdipartimentale NatRisk, Via L. Da Vinci 44, 10095 Grugliasco (TO), Italy.* *http://www.natrisk.org*

∗ Corresponding author. Tel. +39-011-6705296. Fax +39-011-6707615. *davide.vione@unito.it*

Abstract

The UV filter benzophenone-3 (BP3) has UV photolysis quantum yield $\Phi_{BP3} = (3.1\pm0.3)\cdot10^{-5}$ and the following second-order reaction rate constants: with $^{\bullet}OH$, $k_{BP3,{}^{\bullet}OH} = (2.0\pm0.4)\cdot10^{10}$ M^{-1} s^{-1}; with the triplet states of chromophoric dissolved organic matter ($^3CDOM^*$), $k_{BP3,{}^3CDOM^*} = (1.1\pm0.1)\cdot10^9$ M^{-1} s^{-1}; with $^1O_2$, $k_{BP3,{}^1O_2} = (2.0\pm0.1)\cdot10^5$ M^{-1} s^{-1}, and with $CO_3^{-\bullet}$, $k_{BP3,CO_3^{\bullet}} < 5\cdot10^7$ M^{-1} s^{-1}. These data allow the modelling of BP3 photochemical transformation, which helps filling the knowledge gap about the environmental persistence of this compound. Under typical surface-water conditions, direct photolysis and reactions with $^{\bullet}OH$ and $^3CDOM^*$ would be the main processes of BP3 phototransformation. Reaction with $^{\bullet}OH$ would prevail at low DOC, direct photolysis at intermediate DOC (around 5 mg C L^{-1}), and reaction with $^3CDOM^*$ at high DOC. If the reaction rate constant with $CO_3^{-\bullet}$ is near the upper limit of experimental measures ($5\cdot10^7$ M^{-1} s^{-1}), the $CO_3^{-\bullet}$ degradation process could be somewhat important for DOC < 1 mg C L^{-1}. The predicted half-life time of BP3 in surface waters under summertime conditions would be of some weeks, and it would increase with increasing depth and DOC. BP3 transformation intermediates were detected upon reaction with $^{\bullet}OH$. Two methylated derivatives were tentatively identified, and they were probably produced by reaction between BP3 and fragments arising from photodegradation. The other intermediates were benzoic acid (maximum concentration ~10% of initial BP3) and benzaldehyde (1%).

Keywords: Environmental modelling; Surface-water photochemistry; Indirect photolysis; Photosensitisers; Pharmaceuticals and personal care products.

1. Introduction

Benzophenone-3 (2-hydroxy-4-methoxybenzophenone, hereafter BP3) can absorb sunlight in the UVA and UVB regions, with limited phototransformation. This property accounts for its use as sunlight filter in sunbathing lotions and in other cosmetic formulations, to protect either the skin or other formulation components from the effects of sunlight exposure (Rieger, 1997). BP3 is also employed as photostabiliser in packaging materials, to prevent polymer photochemical degradation and in the treatment of photodermatitis. An important consequence of the widespread use of BP3 is its frequent detection in human urine samples (up to 97% samples in the US; Calafat et al., 2008; Krause et al., 2012). BP3 may enter the body principally upon dermal exposure, while the oral intake is much less likely despite the rapid absorption by the gastrointestinal tract. Both phase I and phase II metabolism is observed, which is mostly carried out by liver and kidneys to produce compounds such as 2,4-dihydroxybenzophenone, 2,2'-dihydroxy-4-methoxybenzophenone and 2,3,4-trihydroxybenzophenone. Both the primary compound and its metabolites are excreted in urine in the form of glucuronated derivatives (Okereke et al., 1993; Kadry et al., 1995; Calafat et al., 2008). BP3 has low acute toxicity (Okereke et al., 1995), but it shows estrogenic activity in several fish species, where it acts as vitellogenin inducer (Schlumpf et al., 2001; Schlenk et al., 2005; Kunz et al., 2006; Coronado et al., 2008). Therefore, BP3 has potential to cause feminisation of male fish.

BP3 can reach aquatic systems directly, due to its use as a sunscreen in recreational activities, or through wastewater because of its incomplete elimination in wastewater treatment plants (WWTPs; Balmer et al., 2005; Li et al., 2007). BP3 has been detected at levels of up to some $\mu g\ L^{-1}$ in raw wastewater, at tens to several hundreds $ng\ L^{-1}$ in treated wastewater, and up to a hundred $ng\ L^{-1}$ in lake water (Poiger et al., 2004; Balmer et al., 2005; Rodil et al., 2008). Moreover, it has been detected at $ng\ g^{-1}$ levels in solid matrices and in biota (Meinerling and Daniels, 2006; Nieto et al., 2009). For these reasons, BP3 is considered as a personal care product of emerging environmental concern (Daughton and Ternes, 1999).

To date, very little is known about the environmental persistence of BP3. Its partial elimination in WWTPs (in the 68-96% range; Balmer et al., 2005; Li et al., 2007) suggests that biodegradation would be possible. Direct phototransformation is sufficiently slow to prevent the exploitation of photolysis as a removal technique of BP3 from aqueous solutions (Rodil et al., 2009). However, very little information is available on the photochemical behaviour of BP3 under conditions that are significant for surface waters. In addition to direct photolysis where transformation is induced by sunlight absorption, indirect photochemical pathways are also operational in sunlit water bodies. The latter processes involve reaction between the substrate and reactive transients, most notably $^{\bullet}OH$, $CO_3^{-\bullet}$, $^1O_2$ and the excited triplet states of chromophoric dissolved organic matter, $^3CDOM^*$. These species are generated by sunlight irradiation of photosensitisers such as nitrate, nitrite and CDOM (Boreen et al., 2003; Al Housari et al., 2010). In the case of $CO_3^{-\bullet}$, the formation pathways

include oxidation of bicarbonate and carbonate by $^\bullet$OH and of carbonate by ^{3}CDOM* (Canonica et al., 2005).

This paper has the goal of assessing the photochemical transformation kinetics of BP3 *via* the main photochemical processes that are usually operational in surface waters, namely direct photolysis and reaction with $^\bullet$OH, $CO_3^{-\bullet}$, $^1O_2$ and ^{3}CDOM*. This objective is pursued by combination of laboratory experiments (to determine photolysis quantum yields and second-order reaction rate constants) and of a modelling approach that makes use of kinetic parameters to assess phototransformation rates as a function of water chemical composition and depth. By adopting this methodology (Vione et al., 2010a; Maddigapu et al., 2011; Vione et al., 2011), it is possible to predict the photochemical behaviour of a compound in the environment under conditions that it would be difficult or even impossible to reproduce in the laboratory.

2. Experimental section

2.1. Reagents and materials

Benzaldehyde (purity grade 99%), anthraquinone-2-sulphonic acid, sodium salt (AQ2S, 97%), 1-nitronaphthalene (1NN, 99%), furfuryl alcohol (98%), NaNO$_3$ (>99%), NaHCO$_3$ (98%), anhydrous Na$_2$SO$_4$ (99%), NaCl (99.5%), Na$_2$HPO$_4$ · 2 H$_2$O (98%), NaH$_2$PO$_4$ · H$_2$O (98%), HClO$_4$ (70%) and H$_3$PO$_4$ (85%) were purchased from Aldrich, NaOH (99%), 2-propanol (LiChrosolv gradient grade) and dichloromethane (GC Suprasolv) from VWR Int., benzoic acid (97%) and methanol (gradient grade) from Carlo Erba, Rose Bengal (RB) and 2-hydroxy-4-ethoxybenzophenone (BP3, 98%) from Alfa Aesar.

2.2. Irradiation experiments

The kinetic parameters relevant to the main photochemical processes that would involve BP3 in surface waters (direct photolysis and reaction with $^\bullet$OH, $CO_3^{-\bullet}$, $^1O_2$ and ^{3}CDOM*) were determined by laboratory measurements. These results allow the modelling of BP3 lifetime as a function of environmental variables (Vione et al., 2011; De Laurentiis et al., 2012b). AQ2S was used as CDOM proxy, to assess reactivity between BP3 and ^{3}CDOM*. Reasons for this choice are the widespread occurrence of quinones in CDOM and the fact that irradiation of AQ2S, unlike other triplet sensitisers, does not yield interfering transients such as $^\bullet$OH and $^1O_2$ (Cory and McKnight, 2005; Maddigapu et al., 2010). AQ2S initial concentration was 0.1 mM, to limit the additional complication represented by reaction between ^{3}AQ2S* and ground-state AQ2S (Bedini et al., 2012a).

Solutions to be irradiated (5 mL) were placed inside Pyrex glass cells (4.0 cm diameter, 2.3 cm height, 295 nm cut-off wavelength) and magnetically stirred during irradiation. Irradiation of BP3 + nitrate and of BP3 + nitrate + bicarbonate to study reactions with $^\bullet$OH and $CO_3^{-\bullet}$ was carried out under a Philips TL 01 UVB lamp, with emission maximum at 313 nm. The lamp had 3.0±0.2 W

m^{-2} UV irradiance in the 300-400 nm range, measured with a power meter by CO.FO.ME.GRA. (Milan, Italy) equipped with a UV-sensitive probe. The incident photon flux in solution was actinometrically determined using the ferrioxalate method (Kuhn et al., 2004). By knowing, as a function of wavelength, the fraction of radiation absorbed by $Fe(C_2O_4)_3^{3-}$, the quantum yield of Fe^{2+} photoproduction and the shape of the lamp spectrum (measured with an Ocean Optics USB 2000 CCD spectrophotometer), it is possible to use the measured formation rate of Fe^{2+} to fix the value of the incident spectral photon flux density $p°(\lambda)$. The photon flux of the TL 01 lamp between 300 and 500 nm was $P_o = \int_\lambda p°(\lambda)\,d\lambda = (2.0\pm0.1)\cdot10^{-5}$ Einstein L^{-1} s^{-1}. BP3 direct photolysis and its

transformation photosensitised by AQ2S were studied under a Philips TLK 05 UVA lamp, with emission maximum at 365 nm, 28$\pm$2 W m^{-2} UV irradiance (300-400 nm), and $(2.1\pm0.2)\cdot10^{-5}$ Einstein L^{-1} s^{-1} incident photon flux in solution. The photodegradation of BP3 sensitised by Rose Bengal (RB) via $^1O_2$ was studied under a Philips TL D 18W/16 yellow lamp, with emission maximum at 545 nm and 11$\pm$1 W m^{-2} irradiance in the visible, measured with the CO.FO.ME.GRA. power meter equipped with a probe sensitive to visible radiation.

The choice of the lamps had the purpose of exciting each photosensitiser as selectively as possible. The direct photolysis of BP3 was studied under UVA upon consideration of its absorption spectrum, measured with a Varian Cary 100 Scan UV-Vis spectrophotometer. The same instrument was used to measure the absorption spectra of nitrate, AQ2S and RB. The various emission and absorption spectra are reported in Figure 1. Unless otherwise reported, the initial concentration of BP-3 in the irradiation experiments was 20 µM and the solution pH was around 6.5.

2.3. Monitoring of BP3 transformation

After the scheduled irradiation time, cells were withdrawn from the lamp and the irradiated solutions were analysed by high-performance liquid chromatography (HPLC-UV). The Merck-Hitachi instrument was equipped with autosampler AS2000A (100 µL sample volume), pumps L-6200 and L-6000 for high-pressure gradients, a reverse-phase column Merck LiChrocart RP-C18 packed with LiChrospher 100 RP-18 (125 mm × 4.6 mm × 5 µm), UV-Vis detector L-4200, and control software D-7000 Multi HSM-Manager. Elution used the following grandient (A: CH$_3$OH, B: aqueous H$_3$PO$_4$ at pH 2.8, total flow rate 1.0 mL min^{-1}): 40% A for 9 min, then to 80% A in 1 min and kept for 6 min, down to 40% A in 1 min and kept for 4 min. The retention time of BP3 was 13.9 min, column dead time 0.9 min. Under these conditions, two transformation intermediates of BP3 (benzoic acid and benzaldehyde) coeluted at 6.9 min. Their quantification was achieved by use of authentic standards and by detecting absorbance at 220 nm (benzoic acid absorption maximum) and at 250 nm (benzaldehyde absorption maximum). Concentrations were determined by considering the contribution of each compound to the chromatographic peaks at both wavelengths, according to the Beer-Lambert law. BP3 was quantified at 220 nm due to higher sensitivity.

The time evolution of furfuryl alcohol to quantify the formation rate of $^1O_2$ under the yellow lamp was also monitored by HPLC-UV, as reported in Minella et al. (2011).

2.4. Identification of BP3 transformation intermediates

Intermediate identification was carried out with gas chromatography coupled with mass spectrometry. To this purpose, aqueous solutions after irradiation were extracted with 3 mL dichloromethane, dehumidified with anhydrous Na_2SO_4 and evaporated to dryness. Each sample was reconstructed with 100 µL dichloromethane. The solution was transferred into a vial and injected into a capillary gas chromatograph (Agilent 6890) coupled with a mass spectrometer (Agilent 5973 inert). The injection system used was a Gerstel CIS4 PTV. Initial injection temperature was 40 °C, programmed at 5 °C/s; final temperature was 320 °C, held for 9 min. The injection volume was 2 µL in the splitless mode. The capillary column used was a HP-5MS, 30 m × 0.25 mm × 0.25 µm film thickness. Initial column temperature was 40 °C and it was increased by 15 °C/min to 300 °C. The carrier gas was ultrapure He (1.0 mL/min; SIAD, Bergamo, Italy). The ionisation source worked in the electronic impact (EI) mode and the mass spectrometer worked in the Scan mode from 44 to 450 Th. Identification of spectra was performed by using the Wiley 7n library (Agilent Part No. G1035B).

2.5. Laser flash photolysis measures

Carbonate radical was produced *via* an electron transfer reaction from CO_3^{2-} to the excited state of 1-nitronaphthalene (^{3}1NN), which was generated by laser flash excitation (Brigante et al., 2010). The experiments were carried out using the third harmonic (λ_{exc} = 355 nm) of a Quanta Ray GCR 130-01 Nd:YAG laser system instrument, placed in a right-angle geometry with respect to the monitoring light beam. The single pulses were ca. 9 ns in duration, with an energy of ∼90 mJ/pulse. To avoid photodegradation of the solution due to multiple laser shots, a flow cell was used that was connected to a peristaltic pump, allowing fresh solution to continuously purge the laser-exposed volume.

Transient species produced by the pulsed laser beam were monitored by means of time-resolved absorption spectroscopy, using a detection system consisting of a pulsed xenon lamp (150 W), monochromator and a photomultiplier (1P28). A spectrometer control unit was used for synchronising the pulsed light source and programmable shutters with the laser output. The signal from the photomultiplier was digitised by a programmable digital oscilloscope (HP54522A). A 32 bits RISC processor kinetic spectrometer workstation was used to analyse the digitised signal. Experiments were performed at room temperature (~ 293 K).

In the presence of 0.1 M carbonate, the pseudo-first order decay constant of ^{3}1NN monitored at 620 nm increased from ~ $6.3 \cdot 10^5$ s^{-1} to $2.3 \cdot 10^6$ s^{-1}, and a long-lived transient appeared with a maximum absorption around 600 nm. Such species was identified as the carbonate radical ($CO_3^{-\bullet}$) (Weeks and Rabani, 1966), the decay of which was monitored at 600 nm.

2.6. Kinetic data treatment

The time trend of BP3 under irradiation followed pseudo-first order kinetics. Reaction rates were determined by fitting time evolution data with equations of the form $C_t C_o^{-1} = exp(-k\, t)$, where C_t is the concentration of BP3 at the irradiation time t, C_o its initial concentration, and k the pseudo-first order degradation rate constant. The initial degradation rate is $R_{BP3} = k\, C_o$. The reported errors on the rates ($\pm\sigma$) were derived by curve fitting and depended on the scattering of experimental data around the fit curve. The reproducibility of repeated runs was about 15-20%.

2.7. Photochemical modelling

The photochemical model used in this work predicts phototransformation rate constants and half-life times of dissolved compounds as a function of water chemical composition and depth, based on photochemical kinetics parameters such as photolysis quantum yields and reaction rate constants with photogenerated transients ($^{\bullet}OH$, $CO_3^{-\bullet}$, $^1O_2$ and $^3CDOM^*$). The model takes into account sunlight absorption by water (mostly accounted for by CDOM) and the wavelength-dependent differences of light penetration into the water column. Competition for sunlight irradiance between the main photosensitisers (nitrate, nitrite and CDOM) is also taken into account by the model (Vione et al., 2010b; De Laurentiis et al., 2012a). An important issue is that steady irradiation is usual in laboratory experiments, but one should take into account the variable outdoor irradiance and the day-night cycle. For this reason, the model output uses a standardised time unit (summer sunny day, SSD), equivalent to fair-weather 15 July at 45°N latitude (Sur et al., 2012). The SSD is referred to cloudless sky, thus meteorology issues are not taken into account. Details of model equations are reported as Supplementary Material (hereafter SM). An additional issue is that sunlight is not vertically incident over the water surface. The solar zenith angle should be considered, although refraction deviates the light path in water toward the vertical. Because of this phenomenon, the path length l of light in water is longer than the water depth d: on 15 July at 45°N it is $l = 1.05\, d$ at noon, and $l = 1.17\, d$ at ± 3 h from noon that is a reasonable daily average.

The model has been validated for several pollutants, under a variety of environmental conditions for which field data of photochemical persistence were available (Vione et al., 2010b; Maddigapu et al., 2011; Vione et al., 2011; Sur et al., 2012; De Laurentiis et al., 2012b). This accounts for the use of the model in the present context, to assess the otherwise unknown photochemical persistence of BP3 in sunlit water bodies.

A further issue to be mentioned is that we derived a software application from the model (APEX: Aqueous Photochemistry of Environmentally-occurring Xenobiotics), which is available for free download at *http://chimica.campusnet.unito.it/do/didattica.pl/Quest?corso=7a3d*. APEX was used in this work to plot the graphs of BP3 half-life time *vs.* water parameters, and to get insight into model errors and the seasonal trends of photochemical reactions.
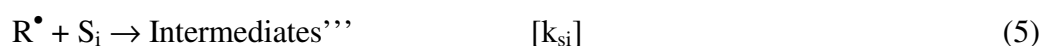
3. Results and Discussion

3.1. Direct photolysis

BP3 (initial concentration 20 µM) was irradiated under the UVA lamp (emission maximum at 365 nm, see Figure 1a) at pH 6.5, for up to 7 days. The substrate followed a pseudo-first order transformation kinetics with $R_{BP3} = (2.69\pm0.26)\cdot10^{-11}$ M s^{-1}. By comparison, BP3 evolution in the dark was negligible. The photon flux absorbed by BP3 was $P_a^{BP3} = \int_{\lambda} p°(\lambda)\,[1-10^{-\varepsilon_{BP3}(\lambda)b[BP3]}]d\lambda =$

$(8.8\pm0.4)\cdot10^{-7}$ Einstein L^{-1} s^{-1}, where $p°(\lambda)$ is the incident spectral photon flux density of the lamp, $\varepsilon_{BP3}(\lambda)$ the molar absorption coefficient of BP3 (see Figure 1a), b = 0.4 cm the optical path length in solution, and [BP3] = 20 µM. From these data it is possible to obtain the polychromatic photolysis quantum yield of BP3 between 300 and 400 nm, where the spectra of the lamp and BP3 overlap, as $\Phi_{BP3} = Rate_{BP3}\,(P_a^{BP3})^{-1} = (3.07\pm0.45)\cdot10^{-5}$.

3.2. Reaction with $^{\bullet}$OH

The reaction rate constant between BP3 and $^{\bullet}$OH was determined upon competition kinetics with 2-propanol, using nitrate UVB photolysis as $^{\bullet}$OH source. Figure 2 reports the initial transformation rate of BP3 (20 µM initial concentration) as a function of the concentration of 2-propanol, upon irradiation of 10 mM nitrate. The alcohol concentration did not exceed the mM range, to avoid interference with the primary steps of nitrate photolysis (Nissenson et al., 2010). The trend of R_{BP3} vs. [2–Propanol] reaches a plateau at high concentration of the alcohol. Based on this behaviour and on previous results obtained with other compounds (Sur et al., 2012), we hypothesise an active contribution to BP3 degradation of radical species ($R^{\bullet}$) that are formed by reaction between 2-propanol and $^{\bullet}$OH. The species $R^{\bullet}$ are expected to react with BP3 (reaction 4) as well as with other components of the system (reaction 5). The transformation of BP3 upon nitrate photolysis would thus proceed as follows (Buxton et al., 1988; Mack and Bolton, 1999):

$NO_3^- + h\nu + H^+ \rightarrow {}^{\bullet}OH + {}^{\bullet}NO_2$	[$\Phi_1 = 0.01$]	(1)
2-Propanol + ${}^{\bullet}OH \rightarrow R^{\bullet}$	[$k_2 = 1.9\cdot10^9$ M^{-1} s^{-1}]	(2)
BP3 + ${}^{\bullet}OH \rightarrow$ Intermediates'	[k_3]	(3)
$R^{\bullet}$ + BP3 $\rightarrow$ Intermediates''	[k_4]	(4)
$R^{\bullet} + S_i \rightarrow$ Intermediates'''	[k_{si}]	(5)

Upon application of the steady-state approximation to $^{\bullet}$OH and $R^{\bullet}$, one gets the expression (6) for the initial transformation rate of BP3 in the presence of 2-propanol, where $R_{\bullet OH}$ is the formation rate of $^{\bullet}$OH in reaction (1) (see SM for the derivation of this equation):

$$R_{BP3} = \frac{R_{\bullet OH} \cdot k_3 \cdot [BP3]}{k_3 \cdot [BP3] + k_2 \cdot [2-\text{Propanol}]} +$$
$$k_4 \cdot [BP3] \cdot \frac{k_2 \cdot [2-\text{Propanol}]}{k_4 \cdot [BP3] + \sum k_{si}[S_i]} \cdot \frac{R_{\bullet OH}}{k_3 \cdot [BP3] + k_2 \cdot [2-\text{Propanol}]} \qquad (6)$$

At very high [2-propanol], reaction (4) prevails over (3) and R_{BP3} becomes:

$$\lim_{High\,[2-\text{Propanol}]} \{R_{BP3}\} = R_{\bullet OH} \frac{k_4 \cdot [BP3]}{k_4 \cdot [BP3] + \sum k_{si}[S_i]} \qquad (7)$$

In contrast, in the absence of 2-propanol one has $R_{BP3} = R_{\bullet OH}$. The fit of experimental rate data with equation (6) (see Figure 2; equation (6) includes (7) in the second term of the sum) yielded $\lim_{High\,[2-\text{Propanol}]} \{R_{BP3}\} = (3.18\pm0.33)\cdot10^{-10}$ M s^{-1}, $R_{\bullet OH} = (5.52\pm0.16)\cdot10^{-9}$ M s^{-1}, and $k_3 = (2.0\pm0.4)\cdot10^{10}$ M^{-1} s^{-1}. The latter is the reaction rate constant between BP3 and $^\bullet$OH.

It should be noted that two additional contributions to the plateau of R_{BP3} *vs.* [2-Propanol] are represented by direct photolysis and reaction with $^\bullet$NO$_2$. However, as reported in paragraph 3.1, the direct photolysis rate of BP3 under the TL01 lamp is around 200 times lower than the degradation rate in the presence of 10 mM nitrate. Therefore, BP3 direct photolysis can be safely neglected under conditions of nitrate irradiation. As far as $^\bullet$NO$_2$ is concerned, phenolic compounds such as BP3 produce nitrophenols upon reaction with nitrogen dioxide. The upper theoretical limit of nitrophenol yield with respect to reacted nitrogen dioxide is 50%, because the nitration process involves two $^\bullet$NO$_2$ (Bedini et al., 2012b). Moreover, there is evidence that the actual yield is not far from the upper limit (Vione et al., 2001). However, the formation of nitrophenols from phenol upon nitrate photolysis accounts for only a few percent of the transformation of the initial substrate, the remainder being accounted for by $^\bullet$OH (Vione et al., 2002). This suggests that the reactivity between $^\bullet$NO$_2$ and phenols is almost negligible compared to the hydroxyl radical. Furthermore, while practically all photogenerated $^\bullet$OH is scavenged by the substrate, a considerable fraction of $^\bullet$NO$_2$ undergoes hydrolysis to nitrate and nitrite (Mack et al., 1996). The fraction of hydrolysed $^\bullet$NO$_2$ is higher at relatively low substrate concentration (Chiron et al., 2007), such as in the present case (20 µM initial BP3), which prevents accumulation of $^\bullet$NO$_2$ in the system and limits the importance of the reactions it takes part into.

3.3. Reaction with CO$_3^{-\bullet}$

The assessment of the reactivity between organic compounds and CO$_3^{-\bullet}$ can be carried out with a semi-quantitative screening method, which makes use of nitrate and bicarbonate under UVB irradiation (Vione et al., 2009). The application of this method (see SM) suggested that the reaction between BP-3 and CO$_3^{-\bullet}$ might possibly be important, which prompted us to use the laser flash photolysis technique to get insight into reaction kinetics. In analogy with the procedure used to

produce other radical species (Sur et al., 2011), $CO_3^{-\bullet}$ was generated by laser excitation of 1NN (reaction 8), leading to the formation of ^{3}1NN followed by electron transfer from carbonate ions to ^{3}1NN (reaction 9):
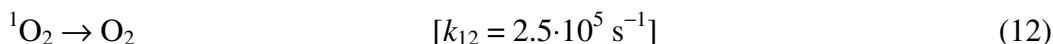
$$1NN + h\nu \rightarrow 1NN^* \xrightarrow{\text{(ISC)}} {}^3 1NN \qquad (8)$$

$$^3 1NN + CO_3^{2-} \rightarrow 1NN^{-\bullet} + CO_3^{-\bullet} \qquad (9)$$

where ISC = inter-system crossing.

In the absence of BP3 the first-order decay constant of $CO_3^{-\bullet}$ was $(9.7\pm0.2)\cdot10^4$ s^{-1}, which was not significantly modified in the presence of 50 μM BP3 (higher concentration values could not be tested because of solubility issues). Based on experimental uncertainty, an upper limit of $5\cdot10^7$ M^{-1} s^{-1} can be derived for the reaction rate constant between BP3 and $CO_3^{-\bullet}$, which is the highest value causing a variation of the $CO_3^{-\bullet}$ decay constant that is still included within experimental errors.

3.4. Reaction with $^1O_2$

Singlet oxygen was generated upon irradiation of Rose Bengal (RB) under a yellow lamp (emission maximum at 545 nm, Figure 1c), with the purpose of achieving selective RB excitation. A linear trend was obtained for the initial BP3 transformation rate, R_{BP3}, upon irradiation of 10 μM RB, as a function of BP3 initial concentration: $R_{BP3} = (1.91\pm0.08)\cdot10^{-6}$ [BP3] (see Figure 3).

Reactions (10-12) would be operational in the irradiated system. In particular, reaction (11) between BP3 and $^1O_2$ would be in competition with the thermal deactivation of singlet oxygen (reaction 12; Rodgers and Snowden, 1982):

$$RB + h\nu + O_2 \rightarrow RB + {}^1O_2 \qquad (10)$$

$$BP3 + {}^1O_2 \rightarrow \text{Intermediates} \qquad [k_{11}] \qquad (11)$$

$$^1O_2 \rightarrow O_2 \qquad [k_{12} = 2.5\cdot10^5 \text{ s}^{-1}] \qquad (12)$$

Upon application of the steady-state approximation to $^1O_2$ one gets the following expression for the initial transformation rate of BP3 (R_{BP3}) (see SM for the derivation of this equation):

$$R_{BP3} = \frac{R_{{}^1O_2} \cdot k_{11} \cdot [BP3]}{k_{12} + k_{11} \cdot [BP3]} \qquad (13)$$

where $R_{{}^1O_2}$ is the formation rate of $^1O_2$ by 10 μM RB under the adopted irradiation device. For very low [BP3] one gets (k_{11} [BP3] « k_{12}):

$$\lim_{[BP3]\rightarrow0} \{R_{BP3}\} = R_{{}^1O_2} \cdot k_{11} \cdot k_{12}^{-1} \cdot [BP3] \qquad (14)$$

10

Equation (14) is consistent with the linear trend of R_{BP3} *vs.* [BP3]. The measurement of $R_{^1O_2}$ was carried out upon irradiation of 10 µM RB + 0.1 mM furfuryl alcohol (FFA), which reacts with $^1O_2$ with rate constant $k_{FFA} = 1.2 \cdot 10^8$ M^{-1} s^{-1} (Wilkinson and Brummer, 1981). Under the adopted experimental conditions, the initial transformation rate of FFA was $R_{FFA} = (1.10\pm0.08) \cdot 10^{-7}$ M s^{-1}. Photogenerated $^1O_2$ could undergo deactivation or reaction with FFA, and upon application of the steady-state approximation to [$^1O_2$] one obtains:

$$R_{^1O_2} = R_{FFA} \cdot \frac{k_{12} + k_{FFA} \cdot [FFA]}{k_{FFA} \cdot [FFA]} \qquad (15)$$

From equation (15) one gets $R_{^1O_2} = (2.40\pm0.17) \cdot 10^{-6}$ M s^{-1}. From equation (14) and $R_{BP3} = (1.91\pm0.08) \cdot 10^{-6}$ [BP3] one derives $R_{BP3}[BP3]^{-1} = R_{^1O_2} k_{11} k_{12}^{-1} = (1.91\pm0.08) \cdot 10^{-6}$. From the known values of $R_{^1O_2}$ and k_{12} one finally obtains $k_{11} = (1.99\pm0.08) \cdot 10^5$ M^{-1} s^{-1} as the reaction rate constant between BP3 and $^1O_2$.

3.5. Reaction with irradiated AQ2S

Anthraquinone-2-sulphonate (AQ2S) was here used as a proxy of chromophoric dissolved organic matter (CDOM), and irradiation was carried out under UVA (see Figure 1a). A linear trend was obtained for the initial transformation rate R_{BP3}, as a function of BP3 initial concentration (the latter was kept below 20 µM), upon UVA irradiation of 0.1 mM AQ2S at pH 6.5: $R_{BP3} = (3.48\pm0.10) \cdot 10^{-5}$ [BP3]. The direct photolysis of BP3 (irradiation without AQ2S) was negligible at the adopted irradiation time scale (up to 8 h).

The triplet state ^{3}AQ2S*, which is the main reactive species of AQ2S under irradiation, has formation quantum yield $\Phi_{^3AQ2S*} = 0.18$ and deactivation rate constant $k_{^3AQ2S*} = 1.1 \cdot 10^7$ s^{-1} (Loeff et al., 1983; Alegría et al., 1999). The formation rate of ^{3}AQ2S* would thus be $R_{^3AQ2S*} = \Phi_{^3AQ2S*} P_a^{AQ2S}$, where P_a^{AQ2S} is the photon flux absorbed by AQ2S (units of Einstein L^{-1} s^{-1}). There would be competition between ^{3}AQ2S* transformation or deactivation and reaction with BP3, which has second-order reaction rate constant $k_{^3AQ2S*,BP3}$. The main processes involved in the irradiation of BP3 + AQ2S are reported in the scheme below, where ISC = inter-system crossing (Bedini et al., 2012a):

$$\text{(16)}$$
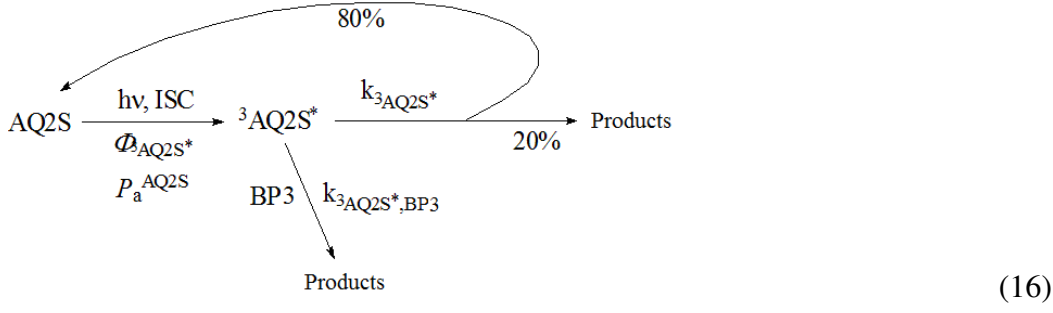
Upon application of the steady-state approximation to ^{3}AQ2S*, the transformation rate of BP3 by irradiated AQ2S can be expressed as follows (see SM for the derivation of this equation):

$$R_{BP3} = \Phi_{^3AQ2S*} \cdot P_a^{AQ2S} \cdot \frac{k_{^3AQ2S*,BP3} \cdot [BP3]}{k_{^3AQ2S*} + k_{^3AQ2S*,BP3} \cdot [BP3]} \qquad (17)$$

Under the hypothesis that $k_{^3AQ2S*,BP3}$ [BP3] « $k_{^3AQ2S*}$, one gets $R_{BP3} = \Phi_{^3AQ2S*} \, P_a^{AQ2S} \, k_{^3AQ2S*,BP3}$ $(k_{^3AQ2S*})^{-1}$ [BP3], which is compatible with the linear trend that was experimentally determined. The quantum yield of BP3 transformation by irradiated AQ2S would be:

$$\Phi_{BP3,AQ2S} = \frac{R_{BP3}}{P_a^{AQ2S}} = \Phi_{^3AQ2S*} \cdot \frac{k_{^3AQ2S*,BP3}}{k_{^3AQ2S*}} \cdot [BP3] \qquad (18)$$

To determine the rate constant $k_{^3AQ2S*,BP3}$, based on equation (18) and the experimental data, one needs to calculate P_a^{AQ2S}. The absorption of radiation by BP3 is not completely negligible compared to 0.1 mM AQ2S. Therefore, to calculate the photon flux absorbed by AQ2S, one should take into account the competition with BP3 for radiation absorption. At any given wavelength λ, the ratio of the spectral photon flux densities absorbed by AQ2S and BP3 ($p_a^{AQ2S}(\lambda)$ and $p_a^{BP3}(\lambda)$, respectively) equals the ratio of the respective absorbances ($A_{AQ2S}(\lambda)$ and $A_{BP3}(\lambda)$) (Braslavsky, 2007). On this basis one can derive the photon flux absorbed by AQ2S, $P_a^{AQ2S} = \int_\lambda p_a^{AQ2S}(\lambda)\,d\lambda$, as follows:

$$P_a^{AQ2S} = \int_\lambda \left[\frac{A_{AQ2S}(\lambda)}{A_{AQ2S}(\lambda) + A_{BP3}(\lambda)} \cdot p^o(\lambda) \cdot (1 - 10^{-(A_{AQ2S}(\lambda) + A_{BP3}(\lambda))}) \right] d\lambda \qquad (19)$$

where $p^o(\lambda) \cdot (1 - 10^{-(A_{AQ2S}(\lambda) + A_{BP3}(\lambda))})$ is the spectral photon flux density absorbed by the solution. At the low concentration values of BP3 used in this work, the trend of calculated P_a^{AQ2S} vs. [BP3] was approximately linear: $P_a^{AQ2S} = \{(2.0\pm0.1)\cdot10^{-6} - (5.4\pm0.4)\cdot10^{-3}$ [BP3]$\}$ Einstein L^{-1} s^{-1}. The experimental data of R_{BP3} vs. [BP3] can be transformed into quantum yields as $\Phi_{BP3,AQ2S} = R_{BP3}$

$(P_a^{AQ2S})^{-1}$, and the values of $\Phi_{BP3,AQ2S}$ *vs.* [BP3] thus obtained are reported in Figure 4. These data can be directly compared with equation (18).

The fit of Figure 4 data with a linear equation yielded $\Phi_{BP3,AQ2S}$ = (18.15±0.55) [BP3]. Upon comparison of this result with equation (18) one obtains $\Phi_{^3AQ2S*}$ $k_{^3AQ2S*,BP3}$ $(k_{^3AQ2S*})^{-1}$ = 18.15±0.55. From the known values $\Phi_{^3AQ2S*}$ = 0.18 and $k_{^3AQ2S*}$ = $1.1 \cdot 10^7$ s^{-1} (Loeff et al., 1983; Alegría et al., 1999), one derives $k_{^3AQ2S*,BP3}$ = (18.15±0.55) $k_{^3AQ2S*}$ $(\Phi_{^3AQ2S*})^{-1}$ = $(1.11 \pm 0.03) \cdot 10^9$ M^{-1} s^{-1} as the reaction rate constant between ^{3}AQ2S* and BP3. This finding confirms that the hypothesis $k_{^3AQ2S*,BP3}$ [BP3] « $k_{^3AQ2S*}$ was reasonable. Hereafter, it will be hypothesised that the value of $k_{^3AQ2S*,BP3}$ is representative of the reaction rate constant(s) between BP3 and the excited triplet states of CDOM (^{3}CDOM*).

3.6. Transformation intermediates

Benzoic acid and benzaldehyde were quantified by liquid chromatography. They were formed as intermediates upon nitrate photolysis ($^\bullet$OH as reactive species) and with nitrate + bicarbonate (involving $^\bullet$OH and/or $CO_3^{-\bullet}$). With nitrate, benzoic acid reached a maximum concentration value of ~1 µM (~5% of the initial 20 µM BP3) and benzaldehyde of ~0.2 µM (~1% of initial BP3). With nitrate + bicarbonate the maximum concentration values were ~2 and ~0.1 µM, respectively (see Figure 5). The two intermediates are likely to derive from bond cleavage between the BP3 carbonyl group and the aromatic ring carrying the hydroxyl and methoxy functions. This process has been reported to play an important role in the phototransformation of BP3 (Liu et al., 2011). Benzoic acid and benzaldehyde were not detected upon BP3 direct photolysis or reaction with ^{1}O$_2$. In the case of ^{3}AQ2S*, chromatographic interferences by AQ2S transformation intermediates prevented the detection of the (however limited, if any) formation of the two compounds.

Further transformation intermediates were determined by GC-MS on the solutions obtained by irradiation of BP3 + nitrate. These compounds were tentatively identified as methylated derivatives of BP3 (see SM). The GC-MS runs gave no results concerning the intermediates from other processes (direct photolysis and reaction with $CO_3^{-\bullet}$, ^{1}O$_2$ and ^{3}AQ2S*).

3.7. Modelling of BP3 phototransformation in surface waters

By using the photochemical kinetics parameters reported in Table 1 for BP3, it is possible to carry out a model assessment of the half-life time of this compound in surface waters, at mid-latitude and in fair-weather summertime. The phototransformation of BP3 under surface-water conditions is mostly accounted for by direct photolysis and reaction with $^\bullet$OH and ^{3}CDOM*. The $^\bullet$OH reaction would account for 25-50% of BP3 transformation. Higher $^\bullet$OH contribution is predicted at low DOC, because dissolved organic matter is an effective $^\bullet$OH scavenger (Brezonik and Fulkerson-Brekken, 1998). Reaction with ^{3}CDOM* would be favoured at high DOC, which implies high

CDOM as well (Oliveira et al., 2006). The relative importance of ^{3}CDOM* would be higher at high depth, because CDOM is a more effective radiation absorber in the bottom layers of a water body compared to *e.g.* nitrate or nitrite (Loiselle et al., 2009). Direct photolysis would always play an important role, but its contribution to BP3 phototransormation would be highest (in the range of 30-50% depending on water depth) at intermediate DOC values (~5 mg C L^{-1}). If one assumes the upper limit of $5 \cdot 10^7$ M^{-1} s^{-1} for the reaction rate constant between BP3 and CO$_3^{-\bullet}$, the process would be secondary but significant at low DOC (< 1 mg C L^{-1}). For higher DOC values, little to negligible BP3 would undergo degradation by reaction with CO$_3^{-\bullet}$.

Figure 6a shows the plot (generated by the *Plotgraph* function of APEX) of the half-life time of BP3 ($t_{1/2}^{BP3}$) as a function of dissolved organic carbon (DOC) and of the path length l of sunlight in water ($l = 1.17 \, d$, where d is the water depth). It is shown that $t_{1/2}^{BP3}$ is of the order of some weeks. Obviously, the lower is $t_{1/2}^{BP3}$, the faster is the rate of photochemical degradation. The $t_{1/2}^{BP3}$ values increase with increasing l (and d as a consequence), because the bottom layers of a deep water body are poorly illuminated by sunlight. The increase of $t_{1/2}^{BP3}$ with increasing DOC is accounted for by: *(i)* $^\bullet$OH scavenging by DOM, and *(ii)* competition for sunlight irradiance between BP3 and CDOM, which inhibits direct photolysis. The two phenomena would not be fully compensated for by enhancement of ^{3}CDOM* reactions at high DOC.

Figure 6b shows $t_{1/2}^{BP3}$ as a function of nitrate and carbonate. Carbonate yields CO$_3^{-\bullet}$ when it is oxidised by $^\bullet$OH or ^{3}CDOM* (Canonica et al., 2005), but it has low to negligible effect on $t_{1/2}^{BP3}$. This is consistent with the limited role of CO$_3^{-\bullet}$ in BP3 degradation, even if the upper limit of $k_{BP3,CO_3^{-\bullet}} = 5 \cdot 10^7$ M^{-1} s^{-1} is taken into account. A similar behaviour is observed when plotting $t_{1/2}^{BP3}$ *vs.* bicarbonate (data not shown). In contrast, the significant decrease of $t_{1/2}^{BP3}$ with increasing nitrate is accounted for by the enhancement of $^\bullet$OH generation under such conditions. Similar results as for nitrate would be observed with nitrite (data not shown).

The uncertainty associated to $t_{1/2}^{BP3}$ depends both on errors in the measured kinetic parameters and on uncertainty in the model equations. For instance, the half-life time of BP3 with $l = 5$ m, DOC = 3 mg C L^{-1}, [NO$_3^-$] = 0.1 mM, [NO$_2^-$] = 1 μM, [HCO$_3^-$] = 1 mM and [CO$_3^{2-}$] = 10 μM is $t_{1/2}^{BP3}$ = 13.3±3.6 SSD (μ±σ). The calculation was carried out with the *APEX_Errors* application of the APEX software.

The results reported so far give insight into BP3 phototransformation under mid-latitude summertime conditions, and the degradation kinetics would obviously be slower in different seasons of the year. Figure 7 reports an approximate assessment of the seasonal trend of $t_{1/2}^{BP3}$ at mid-latitude, made with the *APEX_season* application. It can be seen that $t_{1/2}^{BP3}$ in winter can be 7-9 times higher than in summer (over three months against a couple of weeks, under the same conditions of water chemistry and depth).

An interesting issue is that the second-order reaction rate constants of BP3 with $^\bullet$OH, ^{1}O$_2$ and ^{3}CDOM* are quite similar to those of carbamazepine (CBZ, De Laurentiis et al., 2012; see Table 1). The photolysis quantum yield of BP3 is lower compared to CBZ, but it is compensated for by

higher absorption of sunlight (CBZ absorption is concentrated in the UVB region; De Laurentiis et al., 2012). Because CBZ is a rather refractory pollutant in surface waters (Tixier et al., 2003), it is interesting to compare its photodegradation kinetics with that of BP3. Application of the photochemical model to both compounds suggests that $t_{1/2}^{BP3} \sim 0.5\ t_{1/2}^{CBZ}$, thus meaning that BP3 photodegradation is about twice as fast as that of CBZ. The difference is mostly accounted for by faster direct photolysis of BP3, because of higher sunlight absorption and despite the lower photolysis quantum yield.

The use of BP3 as sunscreen during recreational activities (sunbathing) suggests that an important fraction of this compound would reach seawater, where BP3 has actually been detected (Magi et al., 2012). Two important features of saltwater are much higher ionic strength compared to freshwater (the effect of which cannot be accounted for in the model) and much higher bromide concentration (up to around 1 mM; Jiang et al., 2009). Bromide is the main hydroxyl scavenger in seawater (Buxton et al., 1988; Nakatani et al., 2007). The photochemical model has been validated for brackish water (estuarine areas: Maddigapu et al., 2011; Sur et al., 2012) but not for seawater, thus model results in the latter case should be taken with great caution. Anyway, under the hypothesis that $^\bullet$OH scavenging by bromide is the only important seawater effect, the value of $t_{1/2}^{BP3}$ could be increased by 1.5-2 times compared to freshwater conditions, where $^\bullet$OH scavenging by bromide is negligible compared to scavenging by DOM.

4. Conclusions

The photochemical reactivity data obtained in this work suggest that BP3 in surface waters would mainly be degraded by direct photolysis and reaction with $^\bullet$OH and ^{3}CDOM*. The radical $CO_3^{-\bullet}$ would play at most a secondary role, and reaction with $^1O_2$ would be negligible. Direct photolysis would be the main BP3 photodegradation process for intermediate DOC values (around 5 mg C L^{-1}). Indeed, photolysis would always play a significant role, but $^\bullet$OH reaction would be more important at low DOC and ^{3}CDOM* at high DOC. The half-life time of BP3 in surface waters would be of some weeks during summer (and 7-9 times higher during winter), and it would increase with increasing water depth and increasing DOC. The depth effect is observed because the deeper layers of a water body are poorly illuminated by sunlight, thereby slowing down all photochemical reactions. The DOC effect is accounted for by $^\bullet$OH scavenging by DOM and by competition for sunlight irradiance between BP3 and CDOM, which inhibits direct photolysis.

Some BP3 transformation intermediates were detected upon reaction with $^\bullet$OH. Two methylated isomers were tentatively identified by GC-MS, and it was possible to quantify formation of benzoic acid (produced at a maximum concentration of ~10% of initial BP3) and benzaldehyde (~1% of initial BP3).

It is interesting to compare the photochemical persistence of BP3 with that of the refractory anti-epileptic drug carbamazepine, because the two compounds have similar reaction rate constants

with $^\bullet$OH, ^{3}CDOM* and ^{1}O$_2$. Model results show that BP3 would be significantly less persistent than carbamazepine because of faster direct photolysis ($t_{1/2}^{BP3} \sim 0.5\ t_{1/2}^{CBZ}$). Indeed, although the photolysis quantum yield of BP3 is ~20 times lower compared to carbamazepine, BP3 is able to absorb a significantly higher fraction of the sunlight spectrum.

Finally, although model results for seawater are only indicative and they should be used with great caution (the model has been validated for brackish water but not yet for saltwater), $^\bullet$OH scavenging by bromide in saltwater could increase the half-life time of BP3 by 1.5-2 times compared to the corresponding freshwater conditions.

References

Al Housari F, Vione D, Chiron S, Barbati S. Reactive photoinduced species in estuarine waters. Characterization of hydroxyl radical, singlet oxygen and dissolved organic matter triplet state in natural oxidation processes. Photochem Photobiol Sci 2010;9:78-86.

Alegría AE, Ferrer A, Santiago G, Sepúlveda E, Flores W. Photochemistry of water-soluble quinones. Production of the hydroxyl radical, singlet oxygen and the superoxide ion. J Photochem Photobiol A: Chem 1999;127:57-65.

Balmer ME, Buser HR, Muller MD, Poiger T. Occurrence of some organic UV filters in wastewater, in surface waters, and in fish from Swiss lakes. Environ Sci Technol 2005;39:953-62.

Bedini A, De Laurentiis E, Sur B, Maurino V, Minero C, Brigante M, Mailhot G, Vione D. Phototransformation of anthraquinone-2-sulphonate in aqueous solution. Photochem Photobiol Sci 2012a;11:1445-53.

Bedini A, Maurino V, Minero C, Vione D. Theoretical and experimental evidence of the photonitration pathway of phenol and 4-chlorophenol: A mechanistic study of environmental significance. Photochem Photobiol Sci 2012b;11:418-24.

Boreen AL, Arnold WA, McNeill K. Photodegradation of pharmaceuticals in the aquatic environment: A review. Aquat Sci 2003;65:320-41.

Bouillon RC, Miller WL. Photodegradation of dimethyl sulfide (DMS) in natural waters: Laboratory assessment of the nitrate-photolysis-induced DMS oxidation. Environ Sci Technol 2005;39:9471-7.
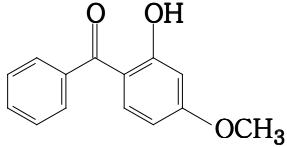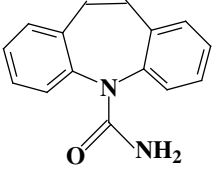
Braslavsky SE. Glossary of terms used in photochemistry, 3rd edition. Pure Appl Chem 2007;79:293-465.

Brezonik PL, Fulkerson-Brekken J. Nitrate-induced photolysis in natural waters: Controls on concentrations of hydroxyl radical photo-intermediates by natural scavenging agents. Environ Sci Technol 1998;32: 3004-10.

Brigante M, Charbouillot T, Vione D, Mailhot G. Photochemistry of 1-nitronaphthalene: a potential source of singlet oxygen and radical species in atmospheric waters. J Phys Chem A 2010;114:2830-6

Buxton GV, Greenstock CL, Helman WP, Ross AB. Critical review of rate constants for reactions of hydrated electrons, hydrogen atoms and hydroxyl radicals ($^\bullet$OH/$^\bullet$O$^-$) in aqueous solution, J Phys Chem Ref Data 1988;17:1027-284.

Calafat AM, Wong LY, Ye X, Reidy JA, Needham LL. Concentrations of the sunscreen agent benzophenone-3 in residents of the United States: National health and nutrition examination survey 2003–2004. Environ Health Perspect 2008;116:893-7.

Canonica S, Kohn T, Mac M, Real FJ, Wirz J, Von Gunten U. Photosensitizer method to determine rate constants for the reaction of carbonate radical with organic compounds. Environ Sci Technol 2005;39:9182-8.

Chiron S, Minero C, Vione D. Occurrence of 2,4-dichlorophenol and of 2,4-dichloro-6-nitrophenol in the Rhône river delta (Southern France). Environ Sci Technol 2007;41: 3127-33.

Coronado M, De Haro H, Deng X, Rempel MA, Lavado R, Schlenk D. Estrogenic activity and reproductive effects of the UV-filter oxybenzone (2-hydroxy-4-methoxyphenyl-methanone) in fish. Aquat Toxicol 2008;90:182-7.

Cory RM, McKnight DM. Fluorescence spectroscopy reveals ubiquitous presence of oxidized and reduced quinones in dissolved organic matter. Environ Sci Technol 2005;39:8142-9.

Daughton CG, Ternes TA Pharmaceuticals and personal care products in the environment: Agents of subtle change? Environ Health Perspect 1999;107:907-38.

De Laurentiis E, Minella M, Maurino V, Minero C, Mialhot G, Sarakha M, Brigante M, Vione D. Assessing the occurrence of the dibromide radical (Br$_2^{-\bullet}$) in natural waters; Measures of triplet-sensitised formation, reactivity, and modelling. Sci Total Environ 2012a;439:299-306.

De Laurentiis E, Chiron S, Kouras-Hadef S, Richard C, Minella M, Maurino V, Minero C, Vione D. Photochemical fate of carbamazepine in surface freshwaters: Laboratory measures and modelling. Environ Sci Technol 2012;46:8164-73.

Jiang XL, Lim LW, Takeuchi T. Determination of trace inorganic anions in seawater samples by ion chromatography using silica columns modified with cetyltrimethylammonium ion. Anal Bioanal Chem 2009;393:387-91.

Kadry AM, Okereke CS, Abdel-Rahman MS, Friedman MA, Davis RA. Pharmacokinetics of benzophenone-3 after oral exposure in male-rats. J Appl Toxicol 1995;15:97-102.

Krause M, Klit A, Jensen MB, Soeborg T, Frederiksen H, Schlumpf M, Lichtensteiger W, Skakkebaek NE, Drzewiecki KT. Sunscreens: are they beneficial for health? An overview of endocrine disrupting properties of UV-filters. Int J Androl 2012;35:424-36.

Kuhn HJ, Braslavsky SE, Schmidt R. Chemical actinometry. Pure Appl Chem 2004;76:2105-46.

Kunz PY, Galicia HF, Fent K. Comparison of in vitro and in vivo estrogenic activity of UV filters in fish. Toxicol Sci 2006;90:349-61.

Li W, Ma Y, Guo C, Hu W, Liu K, Wang Y, Zhu T. Occurrence and behavior of four of the most used sunscreen UV filters in a wastewater reclamation plant. Wat Res 2007;41:3506-12.

Liu YS, Ying GG, Shareef A, Kookana RS. Photostability of the UV filter benzophenone-3 and its effect on the photodegradation of benzotriazole in water. Environ Chem 2011;8:581-8.

Loeff I, Treinin A, Linschitz H. Photochemistry of 9,10-anthraquinone-2-sulfonate in solution. 1. Intermediates and mechanism. J Phys Chem 1983;87:2536-44.

Loiselle SA, Bracchini L, Dattilo AM, Ricci M. The optical characterization of chromophoric dissolved organic matter using wavelength distribution of absorption spectral slopes. Limnol Oceanogr 2009;54:590-7.

Mack J, Bolton JR. Photochemistry of nitrite and nitrate in aqueous solution. J Photochem Photobiol A: Chem 1999;128:1-13.

Maddigapu PR, Bedini A, Minero C, Maurino V, Vione D, Brigante M, Mailhot G, Sarakha M. The pH-dependent photochemistry of anthraquinone-2-sulfonate. Photochem Photobiol Sci 2010;9:323-30.

Maddigapu PR, Minella M, Vione D, Maurino V, Minero C. Modeling phototransformation reactions in surface water bodies: 2,4-Dichloro-6-nitrophenol as a case study. Environ Sci Technol 2011;45:209-14.

Magi E, Di Carro M, Scapolla C, Nguyen, KTN. Stir bar sorptive extraction and LC-MS/MS for trace analysis of UV filters in different water matrices. Chromatographia 75, 973-82.

Mark G, Korth HG, Schuchmann HP, von Sonntag C. The photochemistry of aqueous nitrate ion revisited. J Photochem Photobiol A: Chem 1996;101:89-103.

Meinerling M, Daniels M. A validated method for the determination of traces of UV filters in fish using LC-MS/MS. Anal Bioanal Chem 2006;386:1465-73.

Minella M, Romeo F, Vione D, Maurino V, Minero C. Low to negligible photoactivity of lake-water matter in the size range from 0.1 to 5 μm. Chemosphere 2011;83:1480-5.

Nakatani N, Hashimoto N, Shindo H, Yamamoto M, Kikkawa M, Sakugawa H. Determination of photoformation rates and scavenging rate constants of hydroxyl radicals in natural waters using an automatic light irradiation and injection system. Anal Chim Acta 2007;581:260-7.

Nieto A, Borrull F, Marcé RM, Pocurull E. Determination of personal care products in sewage sludge by pressurized liquid extraction and ultra high performance liquid chromatography-tandem mass spectrometry. J Chromatogr A 2009;1216:5619-25.

Nissenson P, Dabdub D, Das R, Maurino V, Minero C, Vione D. Evidence of the water-cage effect on the photolysis of NO_3^- and $FeOH^{2+}$. Implications of this effect and of H_2O_2 surface

accumulation on photochemistry at the air-water interface of atmospheric droplets. Atmos Environ 2010;44:4859-66.

Okereke CS, Kadry AM, Abdel-Rahman MS, Davis RA, Friedman MA. Metabolism of benzophenone-3 in rats. Drug Metab Dispos 1993;21:788-91.

Okereke CS, Barat SA, Abdel-Rahman MS. Safety evaluation of benzophenone-3 after dermal administration in rats. Toxicol Lett 1995;80:61-7.

Oliveira JL, Boroski M, Azevedo JCR, Nozaki J. Spectroscopic investigation of humic substances in a tropical lake during a complete hydrological cycle. Acta Hydrochim Hydrobiol 2006;34:608-17

Poiger T, Buser HR, Balmer ME, Bergqvist PA, Müller MD. Occurrence of UV filter compounds from sunscreens in surface waters: Regional mass balance in two Swiss lakes. Chemosphere 2004;55:951-63.

Rieger MM. Photostability of cosmetic ingredients on the skin: Disposal of energy by photoactive molecules in sunscreens can adversely affect the sunscreens function and safety. Cosmet Toiletries 1997;112:65.

Rodgers MAJ, Snowden PT. Lifetime of $^1O_2$ in liquid water as determined by time-resolved infrared luminescence measurements. J Am Chem Soc 1982;104:5541-3.

Rodil R, Quintana JB, Lopez-Mahia P, Muniategui-Lorenzo S, Prada-Rodriguez D. Multiclass determination of sunscreen chemicals in water samples by liquid chromatography-tandem mass spectrometry. Anal Chem 2008;80:1307-15.

Rodil R, Moeder M, Altenburger R, Schmitt-Jansen M. Photostability and phytotoxicity of selected sunscreen agents and their degradation mixtures in water. Anal Bioanal Chem 2009;395:1513-24.

Schlenk D, Sapozhnikova Y, Irwin MA, Xie L, Hwang W, Reddy S, Brownawell BJ, Armstrong J, Kelly M, Montagne DE, Kolodziej EP, Sedlak D, Snyder S. In vivo bioassay-guided fractionation of marine sediment extracts from the southern California bight, USA, for estrogenic activity. Environ Toxicol Chem 2005;24:2820-6.

Schlumpf M, Cotton B, Conscience M, Haller V, Steinmann B, Lichtensteiger W. In vitro and in vivo estrogenicity of UV screens. Environ Health Perspect 2001;109:239-44.

Sur B, Rolle M, Minero C, Maurino V, Vione D, Brigante M, Mailhot G. Formation of hydroxyl radicals by irradiated 1-nitronaphthalene (1NN): Oxidation of hydroxyl ions and water by the 1NN triplet state. Photochem Photobiol Sci 2011;10:1817-24.

Sur B, De Laurentiis E, Minella M, Maurino V, Minero C, Vione D. Photochemical transformation of 2-nitro-4-chlorophenol in surface waters: Laboratory and model assessment of the degradation kinetics, and comparison with field data. Sci Total Environ 2012;426:296-303.

Tixier C, Singer HP, Oellers S, Müller SR. Occurrence and fate of carbamazepine, clofibric acid, diclofenac, ibuprofen, ketoprofen, and naproxen in surface waters. Environ Sci Technol 2003;37:1061-8.

Vione D, Maurino V, Minero C, Pelizzetti E. Phenol photonitration upon UV irradiation of nitrite in aqueous solution II: Effects of pH and TiO$_2$. Chemosphere 2001;45:903-10.

Vione D, Maurino V, Minero C, Pelizzetti E. Phenol photonitration. Ann Chim (Rome) 2002;92:919-29.

Vione D, Khanra S, Cucu Man S, Maddigapu PR, Das R, Arsene C, Olariu RI, Maurino V, Minero C. Inhibition vs. enhancement of the nitrate-induced phototransformation of organic substrates by the $^\bullet$OH scavengers bicarbonate and carbonate. Wat Res 2009;43:4718-28.

Vione D, Khanra S, Das R, Minero C, Maurino V, Brigante M, Mailhot G. Effect of dissolved organic compounds on the photodegradation of the herbicide MCPA in aqueous solution. Wat Res 2010a;44:6053-62.

Vione D, Das R, Rubertelli F, Maurino V, Minero C, Barbati S, Chiron, S. Modelling the occurrence and reactivity of hydroxyl radicals in surface waters: Implications for the fate of selected pesticides. Intern J Environ Anal Chem 2010b;90:260-75.

Vione D, Maddigapu PR, De Laurentiis E, Minella M, Pazzi M, Maurino V, Minero C, Kouras S, Richard C. Modelling the photochemical fate of ibuprofen in surface waters. Wat Res 2011;45:6725-36.

Weeks JL, Rabani J. The pulse radiolysis of deaerated aqueous carbonate solutions. I. Transient optical spectrum and mechanism. II. pK for OH radicals. J. Phys. Chem. 70, 2100-2106.

Wilkinson F, Brummer J. Rate constants for the decay and reactions of the lowest electronically excited singlet-state of molecular oxygen in solution. J Phys Chem Ref Data 1981;10:809-1000.

Table 1. Direct photolysis quantum yield (under UVA) and reaction rate constants of BP3 with $^\bullet OH$, $CO_3^{-\bullet}$, $^1O_2$ and $^3AQ2S^*$ (the latter used as a proxy of $^3CDOM^*$). As a comparison, the same parameters are also reported for carbamazepine (De Laurentiis et al., 2012).

| Photochemical parameter	Parameter value	
	S = BP3 (this work)	**S = Carbamazepine (De Laurentiis et al., 2012)**
Φ_S	$(3.1\pm0.3)\cdot10^{-5}$ mole Einstein^{-1}	$(7.8\pm1.8)\cdot10^{-4}$ mole Einstein^{-1}
$k_{S,^\bullet OH}$	$(2.0\pm0.4)\cdot10^{10}$ M^{-1} s^{-1}	$(1.8\pm0.2)\cdot10^{10}$ M^{-1} s^{-1}
$k_{S,CO_3^{-\bullet}}$	$< 5\cdot10^7$ M^{-1} s^{-1}	Negligible
$k_{S,^1O_2}$	$(2.0\pm0.1)\cdot10^5$ M^{-1} s^{-1}	$(1.9\pm0.1)\cdot10^5$ M^{-1} s^{-1}
$k_{S,^3CDOM^*}$	$(1.1\pm0.1)\cdot10^9$ M^{-1} s^{-1}	$(7.0\pm0.2)\cdot10^8$ M^{-1} s^{-1}
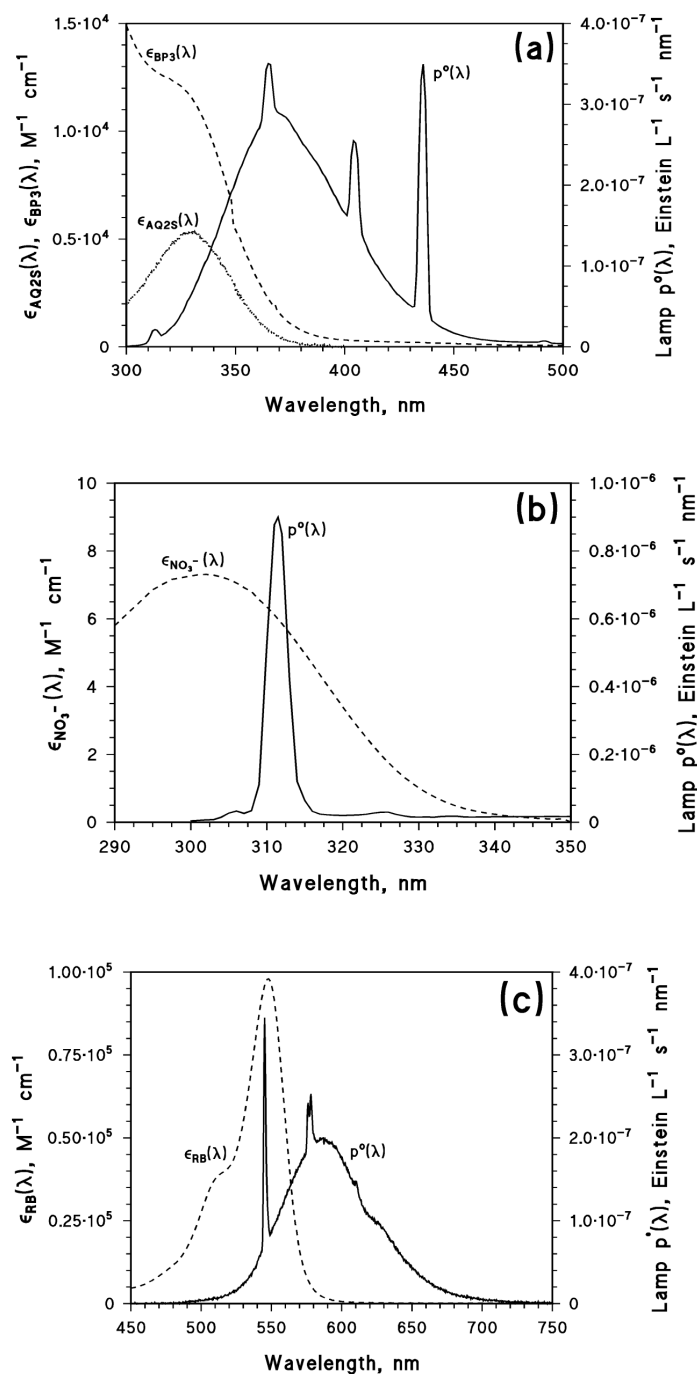
Figure 1. **(a)** Absorption spectra of BP3 and AQ2S (molar absorption coefficients, $\varepsilon_{BP3}(\lambda)$ and $\varepsilon_{AQ2S}(\lambda)$). Spectral photon flux density ($p°(\lambda)$) of the TLK 05 UVA lamp on top of the solutions.

    (b) Absorption spectrum of nitrate (molar absorption coefficient $\varepsilon_{NO3^-}(\lambda)$). Spectral photon flux density ($p°(\lambda)$) of the TL 01 UVB lamp on top of the solutions.

    (c) Absorption spectrum of Rose Bengal (molar absorption coefficient $\varepsilon_{RB}(\lambda)$). Spectral photon flux density ($p°(\lambda)$) of the yellow lamp on top of the solutions.
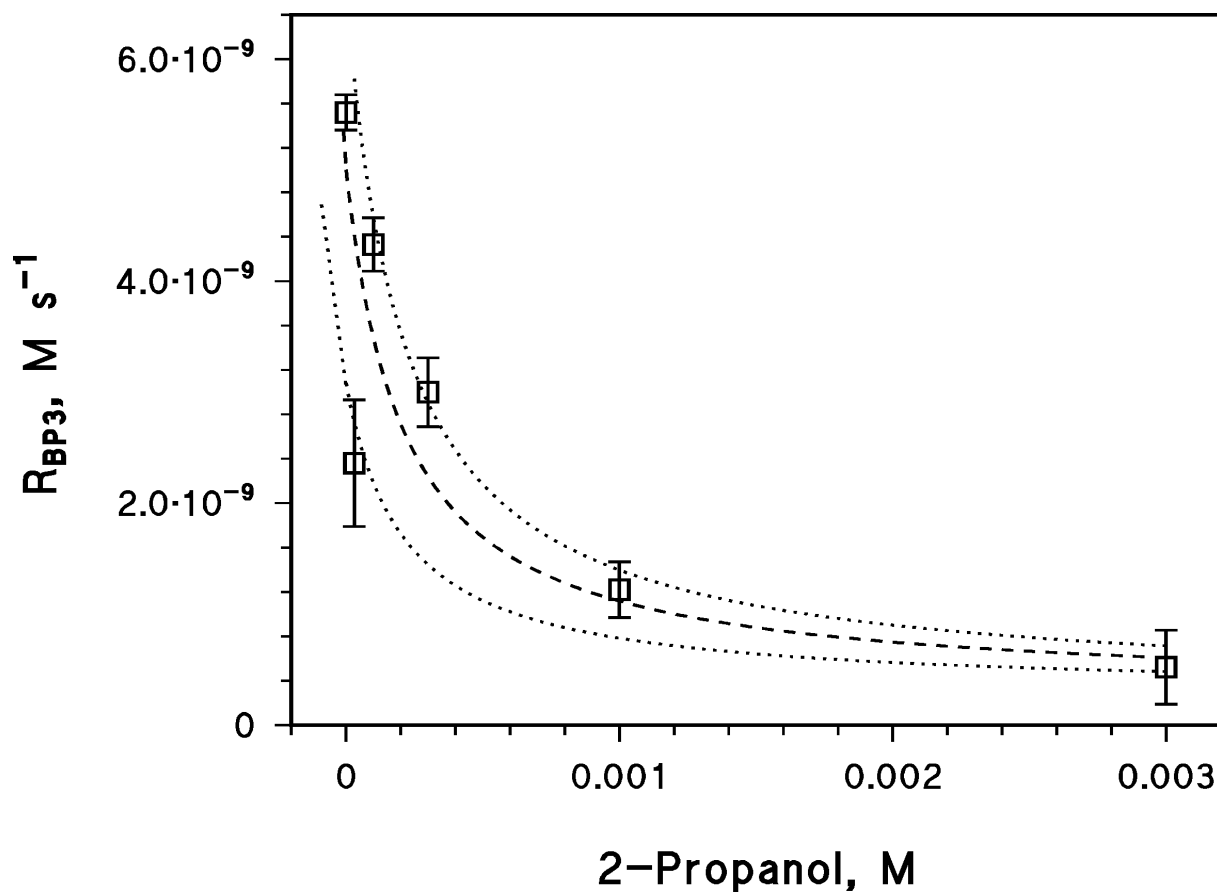
Figure 2. Initial transformation rate of BP3 (R_{BP3}) as a function of the concentration of 2-propanol, upon UVB irradiation of 10 mM $NaNO_3$ at pH 6.5. The dashed curve is the fit of the experimental data with equation (6), the dotted ones are the 95% confidence bands of the fit.
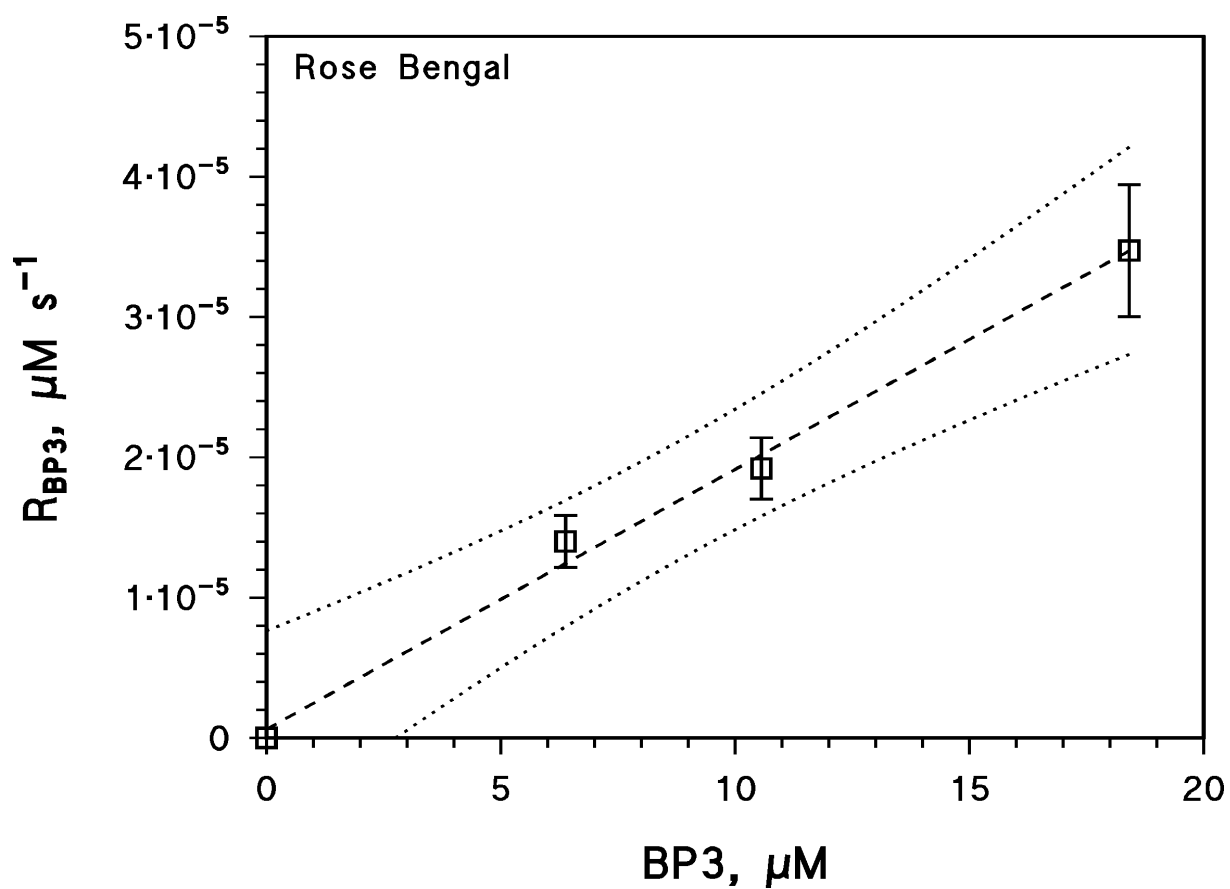
Figure 3. Trend of the initial transformation rate of BP3, R_{BP3}, upon yellow-lamp irradiation of 10 µM RB at pH 6.5, as a function of BP3 initial concentration. The fit line is dashed, the 95% confidence bands are dotted.
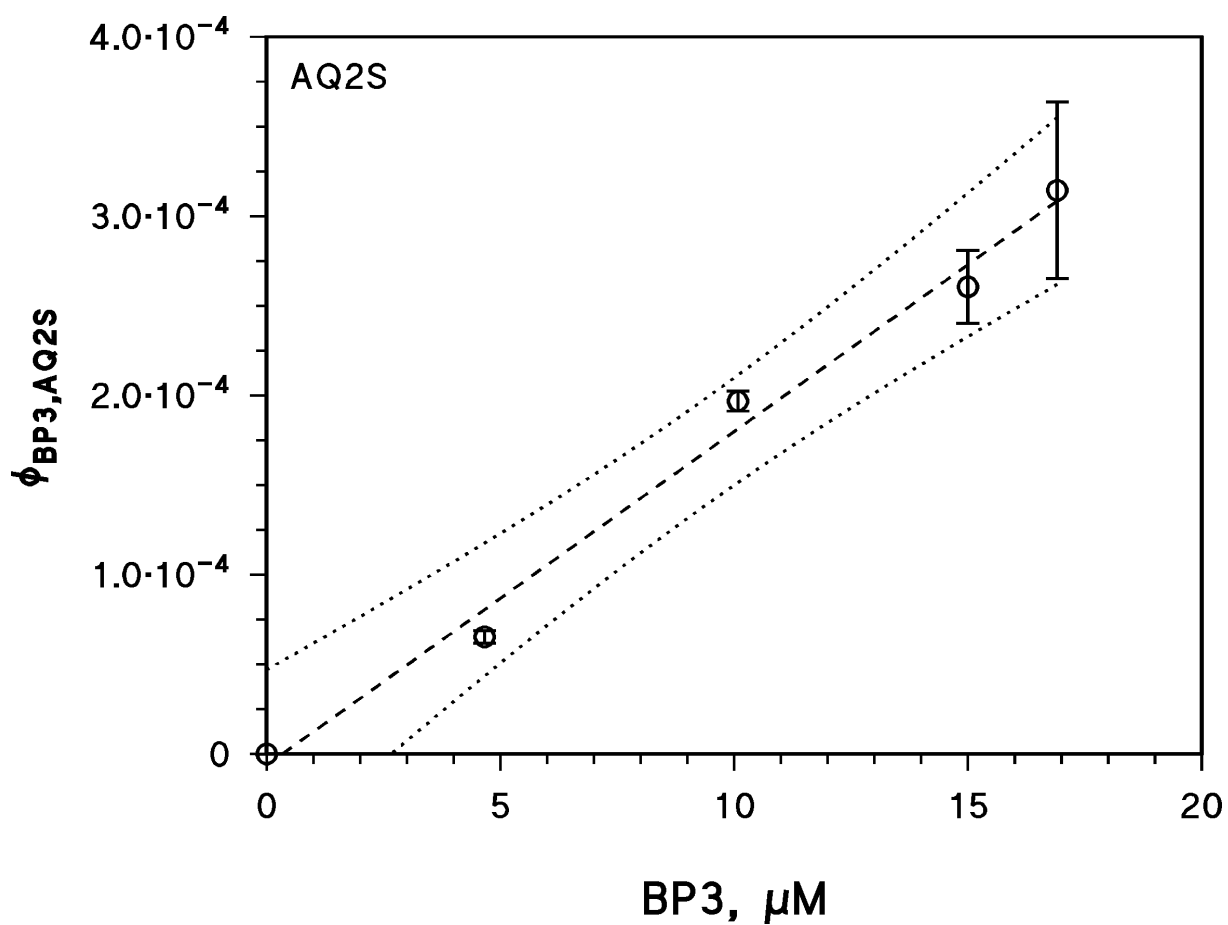
Figure 4. Quantum yield of BP3 transformation upon UVA irradiation of 0.1 mM AQ2S at pH 6.5, as a function of the concentration of BP3. The fit line is dashed, the 95% confidence bands are dotted.
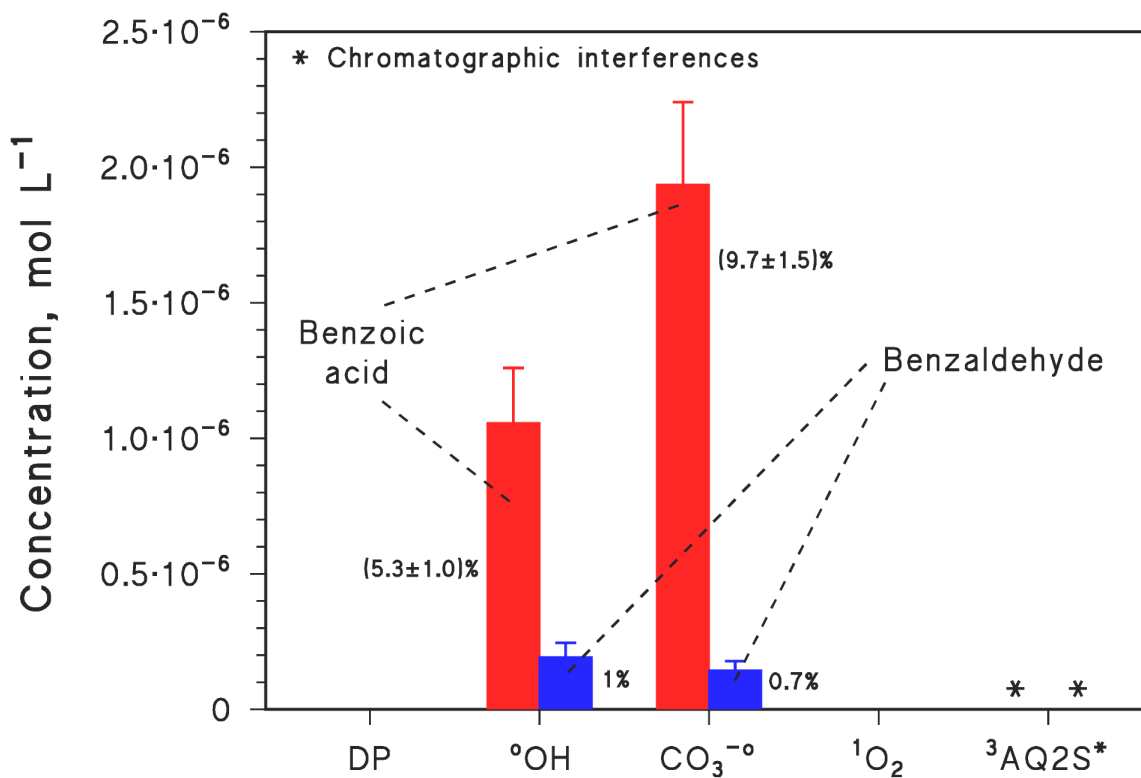
Figure 5. Maximum concentration values reached by benzoic acid and benzaldehyde upon irradiation of 20 µM BP3 alone (DP = direct photolysis) and of 20 µM BP3 in the presence of 10 mM nitrate ($^{\bullet}OH$), 10 mM nitrate + 10 mM bicarbonate ($CO_3^{-\bullet}$), 10 µM RB ($^1O_2$) and 0.1 mM AQ2S ($^3AQ2S^*$). The percentages reported near the bars represent the fraction of initial BP3 that is accounted for by the maximum concentration of the detected intermediate. Error bounds represent $\mu \pm \sigma$.
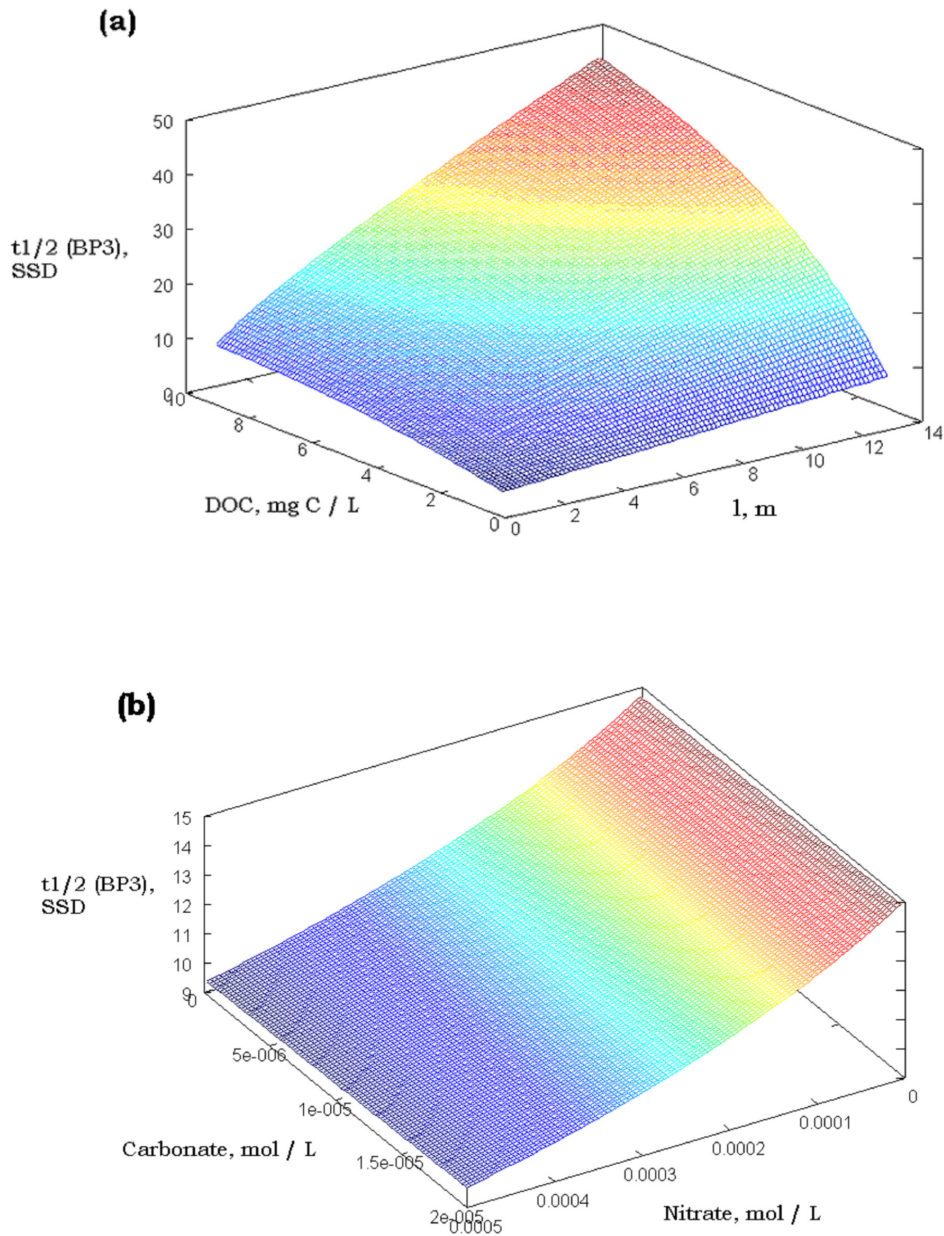
Figure 6. (a) BP3 half-life time as a function of sunlight optical path length in water (*l*) and of dissolved organic carbon (DOC). Other conditions: 0.1 mM nitrate, 1 µM nitrite, 1 mM bicarbonate, 10 µM carbonate. On 15 July at 45°N latitude (conditions relevant to a SSD) one has *l* = 1.17 *d* at ±3h from noon, which can be assumed as a reasonable daily average. Therefore, *l* = 14 m corresponds to *d* = 12 m.

(b) BP3 half-life time as a function of nitrate and carbonate. Other conditions: 0.1 mM nitrate, 1 mM bicarbonate, 3 mg C L^{-1} DOC, and *l* = 5 m (corresponding to *d* = 4.3 m).
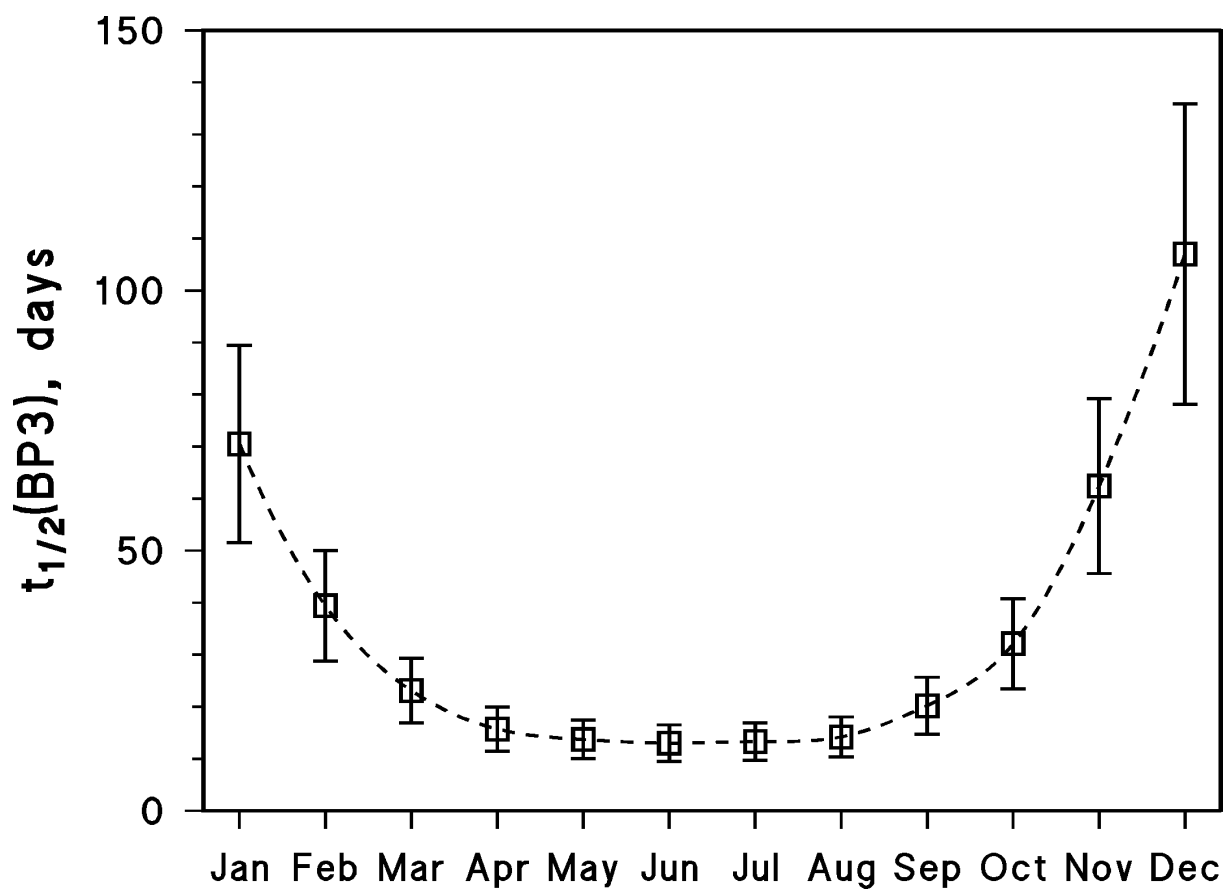
Figure 7. Seasonal trend of the half-life time of BP3 under mid-latitude conditions (45°N), calculated with the *APEX_season* application of the APEX software (*http://chimica.campusnet.unito.it/do/didattica.pl/Quest?corso=7a3d*).

Water parameters: $l = 5$ m, DOC = 3 mg C L^{-1}, [NO$_3^-$] = 0.1 mM, [NO$_2^-$] = 1 μM, [HCO$_3^-$] = 1 mM and [CO$_3^{2-}$] = 10 μM.